

BRIEF PAPER

A 0.4–1.2 GHz Reconfigurable CMOS Power Amplifier for 802.11ah/af Applications

Jaeyong KO^{†a)}, Member and Sangwook NAM^{††}, Nonmember

SUMMARY A reconfigurable broadband linear power amplifier (PA) for long-range WLAN applications fabricated in a 180 nm RF CMOS process is presented here. The proposed reconfigurable in/output matching network provides the PA with broadband capability at the two center frequencies of 0.5 GHz and 0.85 GHz. The output matching network is realized by a switchable transformer which shows maximum peak passive efficiencies of 65.03% and 73.45% at 0.45 GHz and 0.725 GHz, respectively. With continuous wave sources, a 1-dB bandwidth (BW_{1-dB}) according to saturated output power is 0.4–1.2 GHz, where it shows a minimum output power with a power added efficiency (PAE) of 25.62 dBm at 19.65%. Using an adaptive power cell configuration at the common gate transistor, the measured PA under LTE 16-QAM 20 MHz (40 MHz) signals shows an average output power with a PAE exceeding 20.22 (20.15) dBm with 7.42 (7.35)% at an $ACLR_{E-UTRA}$ of -30 dBc, within the BW_{1-dB} .

key words: broadband, CMOS, IEEE 802.11ah/af standards, reconfigurable transformer, power amplifier

1. Introduction

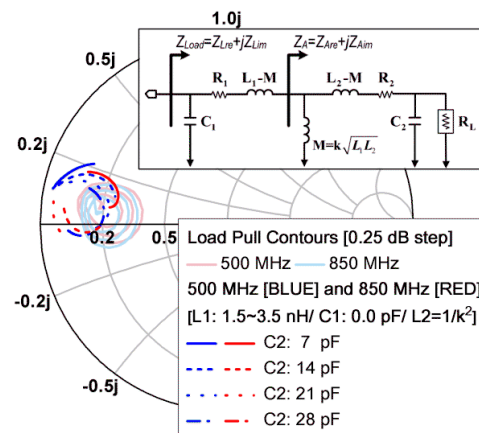
With the development of smart home, Machine-to-Machine (M2M) and the Internet-of-Things (IoT), there has been a great deal of interest in expanding research on the ISM bands [1]. Despite the rapid development of IEEE 802.11 devices on the 2.4 GHz frequency band and IEEE 802.15.4-based sensor devices at ultrahigh frequencies, the spectrum below 1 GHz has also been the subject of new attraction in both the research and standardization areas due to its license-exempt status, lower obstruction losses and longer communication distances.

The IEEE 802.11ah/af standards (470–698 MHz/755–928 MHz) offer WiFi-like experience with reasonable data rates up to and beyond one kilometer [2], [3]. However, the operation frequencies of 802.11ah/af are too broad for one integrated PA to cover. Although several approaches have been developed to achieve broadband behavior with high output power [7], [8], they cannot be applied to the 802.11ah systems. Therefore, a reconfigurable operation in the PA is required to achieve a broader bandwidth. In this Letter, a switchable balun/transformer (TF) is employed as an in/output matching network of the PA, thus offering two modes of operation; Lower frequency mode (LFM): 0.4–0.6 GHz, Higher frequency mode (HFM): 0.6–1.1 GHz. The

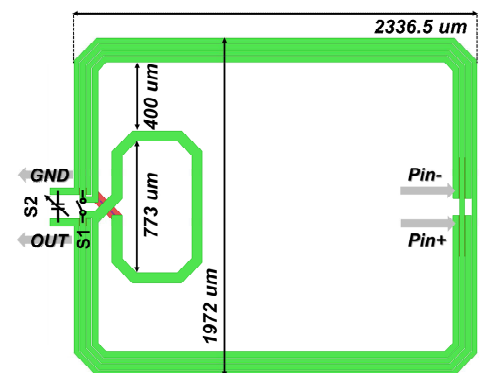
fabricated CMOS PA shows a 1-dB bandwidth (BW_{1-dB}) of 0.4–1.2 GHz under continuous wave (CW) measurements. Within the BW_{1-dB} , the PA generates an average output power (P_{AVG}) which exceeds 20.22 (20.15) dBm below an $ACLR_{E-UTRA}$ of -30 dBc for LTE 16-QAM 20 MHz (40 MHz) signals.

2. Circuit Design of the Reconfigurable Broadband Linear PA

Considering load-pull contours performed at 0.5 GHz and 0.85 GHz (Fig. 1 (a)), the output matching network (OMN) requires a smaller shunt inductor to resonate with the device output capacitance as the frequency increases.



(a)



(b)

Fig. 1 (a) Normalized Z_{Load} with variations of L_1 , L_2 and C_2 at 0.5 GHz and 0.85 GHz, and (b) physical layout of the designed OMN.

Manuscript received July 2, 2018.

Manuscript revised September 2, 2018.

[†]The author is with Samsung Electronics, Suwon, Korea.

^{††}The author is with the Institute of New Media and Communication (INMC), School of Electrical and Computer Engineering, Seoul National University, Seoul, 151-742 Korea.

a) E-mail: james86.ko@samsung.com

DOI: 10.1587/transele.E102.C.91

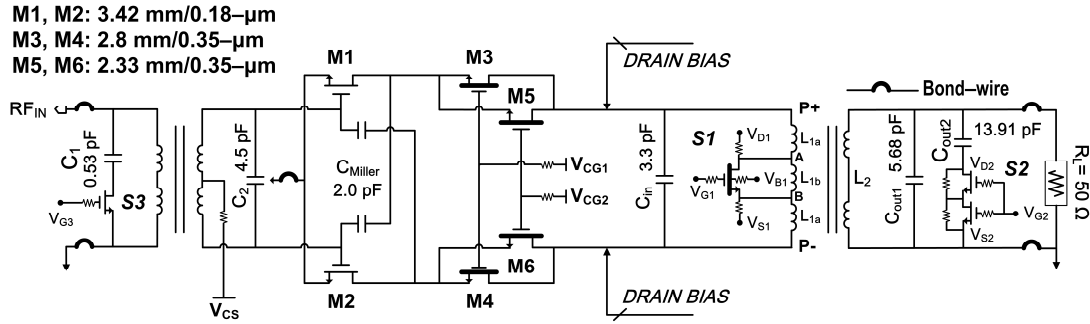


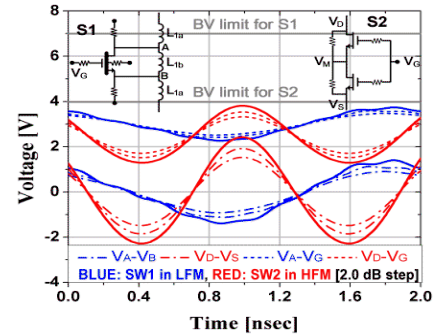
Fig. 2 Overall schematic of the reconfigurable broadband PA.

As illustrated in Fig. 1 (a), the OMN employs an equivalent circuit of a high-Q TF and additional capacitors (C_1 , C_2). Given that the coupling factor is 0.75 and the quality factor is 10, transformed load impedance (Z_{Load}) was simulated as follows: trajectories of Z_{Load} are drawn by varying the primary winding inductance (L_1) and C_2 from 1.5 nH to 3.5 nH and from 7.0 pF to 28.0 pF (increments of 7.0 pF), respectively, at both 0.5 GHz and 0.85 GHz. Figure 1 (a) shows that the real part of Z_{Load} increases with the higher L_1 , whereas C_2 provides precise control of Z_{Load} to the load pull contours. From the calculations, higher and lower values of L_1 (2.75 nH and 2.56 nH) and C_2 (23.5 pF and 9.44 pF) are required at 0.5 GHz and 0.85 GHz, respectively, while the C_1 (0.0 pF) and L_2 (5.03 nH) values are fixed at both frequencies.

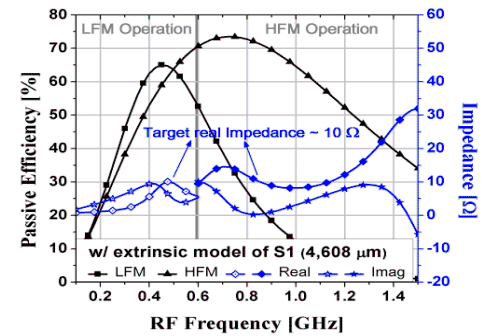
The designed reconfigurable OMN is presented in Fig. 1 (b); L_1 increases with the LFM owing to the inner turn winding while C_2 decreases for the HFM due to the OFF-capacitance (C_{OFF}) of S2. To ensure proper operations, S1 and S2 are turned OFF and ON for the LFM, respectively, while they are correspondingly turned ON and OFF for the HFM. To avoid the effect of parasitic capacitance between the outer and inner primaries, a gap of 400 μm exists, maintaining high passive efficiency of the HFM. Figure 2 presents an overall schematic of the proposed PA, with S1 (4.608 mm/0.35- μm) and S2 (2.304 mm/0.18- μm) implemented by a thick gate-oxide transistor and two stacked transistors, respectively.

As illustrated in Fig. 3 (a), the switches possess power-handling capability in the OFF-state. With corresponding C_{OFF} and R_{on} of 1.61 pF and 0.36 Ω for the S1, the peak passive efficiencies of the OMN are 65.03% and 73.45% for LFM and HFM operations, respectively, as shown in Fig. 3 (b). Also considering a C_{OFF} of 0.61 pF for the S2, the designed Z_{Load} values are 9.58+j4.75 Ω and 10.09+j0.34 Ω at 0.5 GHz and 0.85 GHz, respectively, well within the load-pull contours, as presented in Fig. 4 (a).

To achieve higher linearity for the HFM, an adaptive power cell configuration at the common gate (CG) power cell is applied with a different bias condition (V_{CG1} : 2.36 V, V_{CG2} : 2.06 V) [6]. When the PA operates in lower power region, the CG1 (M3, M4) turns on first. As the input power increases, the source voltage of the CG becomes lower and CG2 (M5, M6) also turns on. This proceeds that the in-

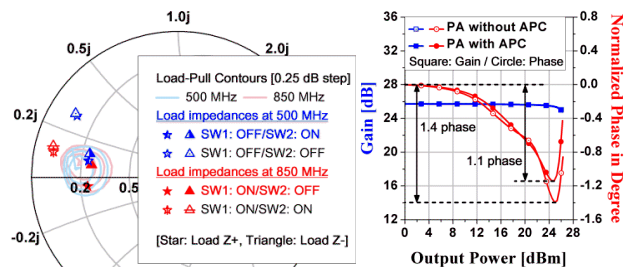


(a)



(b)

Fig. 3 (a) Simulated voltage difference waveforms of S1 and S2 in the OFF-state, and (b) passive efficiencies and complex Z_{Load} depending on the mode operation.



(a)

(b)

Fig. 4 (a) Normalized Z_{Load} of the proposed OMN according to various modes of the switches, and (b) simulated AM-PM distortion results at 0.85 GHz.

put average capacitance variation of each CG has a different sign and the total average capacitance variation can become small due to mutual cancelling. Thus, phase distortion is compensated by 0.3° at 0.85 GHz, as shown in Fig. 4 (b). In addition, a P_{AVG} at -30 dBc is improved by 0.3 dB for two-tone simulations with a tone spacing of 40 MHz.

3. Measurement Results

Figure 5 (a) shows a microphotograph of the proposed PA implemented in the $0.18\text{-}\mu\text{m}$ 1P6M RF CMOS process. With a drain bias of 3.0 V, the PA consumes 440 mA and 430 mA of quiescent current for the LFM and HFM, respectively. With the help of a switchable input balun, the measured peak small-signal gains achieved are 22.0 dB and 24.51 dB at 0.58 GHz and 0.8 GHz, respectively, as depicted in Fig. 5 (b). For the third-order harmonic of the HFM (around the ISM band), the small-signal gain presents lower than -20 dB and the signals can be filtered by duplexers before antennas.

As illustrated in Fig. 6, a $BW_{1\text{-dB}}$ range according to CW measurements is 0.4–1.2 GHz, generating an output power with a power added efficiency (PAE) of more than 25.62 dBm at 19.65%. For LTE 16-QAM 20 MHz/40 MHz signals (PAPR: 7.6 dB), the PA when reconfigured achieves a P_{AVG} of more than 20.22 dBm/20.15 dBm, while its PAE

exceeds 7.42%/7.35% at an $ACLR_{E\text{-}UTRA}$ of -30 dBc, as shown in Fig. 7.

Figure 8 shows the measured output spectrum at 0.5 GHz and 0.85 GHz with channel bandwidths of 10, 20, and 40 MHz. Table 1 summarizes the comparison with previous reported broadband CMOS PAs performing at sub-GHz. Since the proposed PA shows the most broadband characteristic with high linear output power (> 21.5 dBm), this amplifier is sufficiently suitable for use in WLAN 802.11af/ah transceivers.

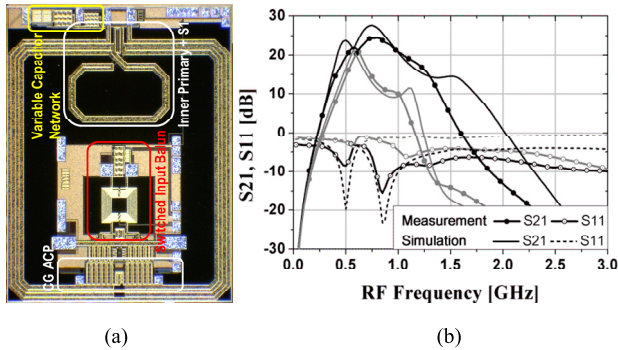


Fig. 5 (a) Chip microphotograph of the CMOS PA (size= 2.62×1.97 mm²), and (b) simulated/measured S-parameter for each mode operation.

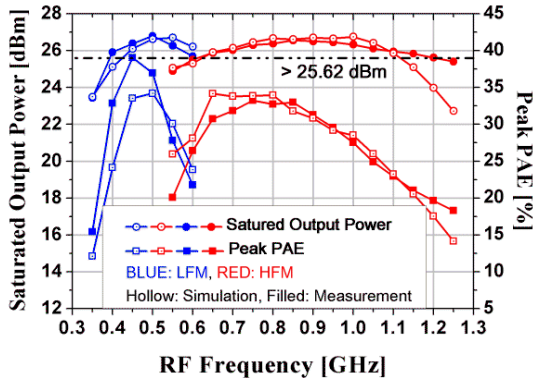


Fig. 6 Simulated/measured saturated output power and peak PAE versus the RF frequencies.

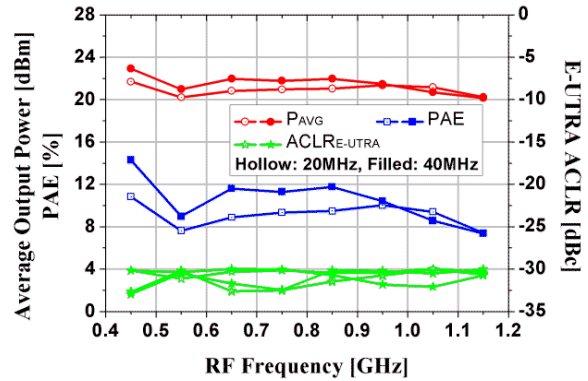
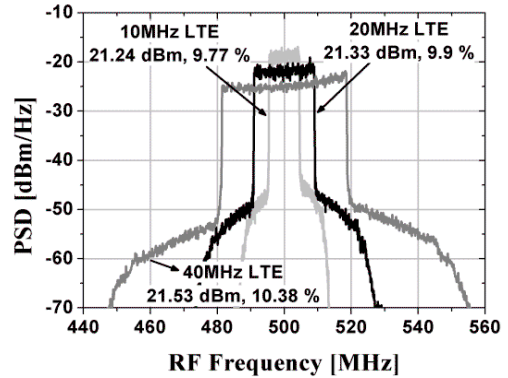
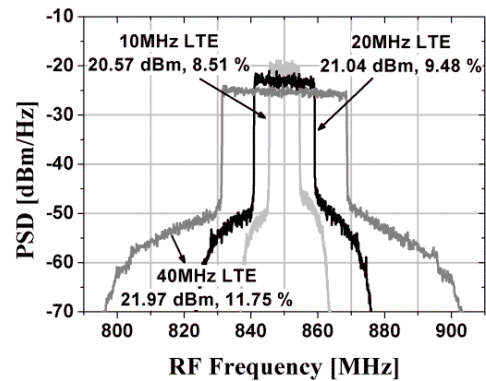


Fig. 7 Measured LTE 16-QAM 20- and 40-MHz performances from 0.45 to 1.15 GHz.



(a)



(b)

Fig. 8 Measured output power spectrum of the PA using 10-, 20- and 40-MHz LTE 16-QAM signals centered at (a) 0.5 GHz and (b) 0.85 GHz.

Table 1 Comparison of broadband CMOS PAs performing at sub-GHz

Reference	Bandwidth [GHz]	Peak PAE [%]	Linearity [dBm/%]	Tech. [nm]	VDD [V]	OMN Integration
[4]	0.38–0.7 (> 20.0 dBm)	46	N/A	180	N/A	NO
[5]	0.7–1.0 (> 13.6 dBm)	25.5	³ 8.9 / – @-37.4 dBc	180	2.0	NO
[6]	N/A	53.5	⁴ 18.2 / –, ⁵ 18.4 / – @2% EVM	40	N/A	NO
[7]	² 0.75–1.23 (> 26.0 dBm)	25.8	⁶ 25.1 / 15.0 @-25 dB EVM	90	2.0	YES
[8]	0.7–1.2 (> 20.1 dBm)	48.3	N/A	130	4.8	YES
This work	0.4–1.2 (> 25.62 dBm)	36.96	⁷ 21.53 / 10.38 ⁸ 21.97 / 11.75 @-30 dBc	180	3.0	YES

¹Values are P1dB. ²Values taken from Fig. 10 in earlier work [7]. ³LTE 16-QAM 5 MHz at 0.7 GHz. 802.11n 64-QAM 20 MHz at ⁴0.65 GHz and ⁵0.88 GHz. ⁶LTE 16-QAM 10 MHz at 0.93 GHz. LTE 16-QAM 40 MHz at ⁷0.5 GHz and ⁸0.85 GHz.

4. Conclusion

This work demonstrates a reconfigurable broadband CMOS PA which targets long-range WLAN applications. The PA operating in two modes incorporates an integrated switchable balun/transformer for an in/output matching network. The OMN provides optimal loads and high passive efficiencies for each mode. Using CW sources, the measured BW_{1-dB} depending on saturated output power shows 0.4–1.2 GHz, presenting an output power with a PAE higher than 25.62 dBm at 19.65%. Under LTE 16-QAM 20 (40) MHz measurements within the BW_{1-dB} , the PA generates a minimum P_{AVG} of 20.22 (20.15) dBm with an $ACLR_{E-UTRA}$ of –30 dBc. These results validate that the suggested design can deliver a linear amplification for a broadband/wideband signal of sub-GHz long-range wireless applications.

Acknowledgments

This work was supported by a grant from the National Research Foundation of Korea (NRF) funded by the Korean government (MSIP). (No. 2016R1E1A1A01943375)

References

- [1] J. van Sinderen, G.W. de Jong, F. Leong, X. He, M. Apostolidou, H.K. Subramanian, R. Rutten, J. Niehof, J. Verlinden, H. Wang, A. Hoogstraate, K.C. Kwok, R. Verlinden, R. Hoogendoorn, D. Jeurissen, A. Salfelner, E. Bergler, J.M.V. Torres, C.J. Haji-Michael, T. Unterweger, E. Tarvainen, M. Posch, R. Schmidt, M. Stattmann, J. Tyminski, P. Jean, S. Darfeuille, O. Aymard, A.L. Grontec, C. Boucey, C. Kelma, and G. Monnerie, "Wideband UHF ISM-band transceiver supporting multichannel reception and DSSS modulation," Proc. IEEE Int. Solid-State Circuits Conf. Tech. Dig., pp.454–456, Feb. 2013.
- [2] S. Aust, R.V. Prasad, and I.G.M.M. Niemegeers, "IEEE 802.11ah: Advantages in standards and further challenges for sub 1 GHz Wi-Fi," 2012 IEEE International Conference on Communications (ICC), pp.6885–6889, June 2012.
- [3] W. Sun, M. Choi, and S. Choi, "IEEE 802.11ah: A long range 802.11 WLAN at sub 1 GHz," Journal of ICT Standardization, vol.1, no.1, pp.83–108, April 2013.
- [4] J. Hur, O. Lee, C.-H. Lee, K. Lim, and J. Laskar, "A multi-level and multi-band class-D CMOS power amplifier for LINC system in the cognitive radio application," IEEE Microw. Wireless Compon. Lett., vol.20, no.6, pp.352–354, June 2010.
- [5] X. Yu, M. Wei, Y. Song, Z. Wang, and B. Chi, "A PAPR-aware dual-mode subgigahertz CMOS power Amplifier for short-range wireless communication," IEEE Trans. Circuits Syst. II Express Briefs, vol.63, no.1, pp.44–48, Jan. 2016.
- [6] B. Kim, D.-H. Lee, S. Hong, and M. Park, "A multi-band CMOS power amplifier using reconfigurable adaptive power cell technique," IEEE Microw. Wireless Compon. Lett., vol.26, no.8, pp.616–618, Aug. 2016.
- [7] B. Francois and P. Reynaert, "A fully integrated watt-level linear 900-MHz CMOS RF power amplifier for LTE-applications," IEEE Trans. Microw. Theory Techn., vol.60, no.6, pp.1878–1885, June 2012.
- [8] K.K. Sessou and N.M. Neihart, "An integrated 700–1200 MHz class-F PA with tunable harmonic terminations in 0.13- μ m CMOS," IEEE Trans. Microw. Theory Techn., vol.63, no.4, pp.1315–1323, April 2015.